Journal of The Electrochemical Society, **156** (8) G109-G113 (2009)
0013-4651/2009/156(8)/G109/5/$25.00 © The Electrochemical Society

$HfO_2/HfO_xN_y/HfO_2$ Gate Dielectric Fabricated by In Situ Oxidation of Plasma-Enhanced Atomic Layer Deposition HfN Middle Layer

W. J. Maeng,[a] Gil Ho Gu,[a] C. G. Park,[a] Kayoung Lee,[b] Taeyoon Lee,[b] and Hyungjun Kim[a,*,z]

[a]*Department of Materials Science and Engineering, Pohang University of Science and Technology, Pohang 790-784, Korea*
[b]*Nanobio Fusion Device Laboratory, School of Electrical and Electronic Engineering, Yonsei University, Seoul 120-749, Korea*

By using H_2 plasma as a reactant with tetrakis(dimethylamino)hafnium precursor during plasma-enhanced atomic layer deposition, we deposited the HfO_xN_y layer between HfO_2 layers. The 5 nm thick $HfO_2/HfO_xN_y/HfO_2$ (HfONO) trilayer gate oxide shows reduced capacitance equivalent oxide thickness (≅1.25 nm) than that (≅1.40 nm) of the HfO_2 film with the same thickness due to the contribution of nitrogen incorporation to the high dielectric constant. The HfONO film utilizing H_2 plasma shows lower values of interface trap density (D_{it}), trapped positive charge density (ΔN_p), and gate leakage currents than the HfO_2 layer with the same thickness while maintaining comparable hysteresis (≤30 mV). The results can be attributed to the presence of N–H bonds, which can reduce localized states below the conduction band and prevent the conduction-band lowering, and decrement of N–N and N–O bonds, which contribute to trap density, confirmed by the combination of X-ray photoelectron spectroscopy and near-edge X-ray absorption fine-structure analyses.
 [DOI: 10.1149/1.3147254]

Manuscript submitted December 15, 2008; revised manuscript received March 2, 2009. Published June 10, 2009.

The incorporation of nitrogen atoms to gate oxide produces beneficial effects, such as the reduction in leakage currents and improvements of the reliability by passivating oxygen vacancy states and enhancing structural stability.[1,2] Conventionally, the nitrogen incorporation into gate oxide has been carried out by high temperature or plasma annealing under a nitrogen environment. In previous results, high process temperatures over 700°C were usually required for nitridation.[3,4] Moreover, a large amount of nitrogen incorporation at the interface between channel region and gate oxide induced large flatband voltage shift, resulting in the mobility degradation.[5] For example, the plasma-nitrided HfO_xN_y has shown a negative voltage shift ($\Delta V_{FB} = -80$ mV) in spite of reliability enhancement.[6] Also, thermal nitridation by NH_3 has shown a large V_{FB} shift ($\Delta V_{FB} = -500$ mV) with 200 mV hysteresis.[3] To solve these problems, a postdeposition nitridation process has been suggested.[3,4] But this method requires high temperature and multiple steps; besides, there is a difficulty in controlling nitrogen profile with atomic accuracy. Thus, the controllable manipulation of nitrogen incorporation into the dielectrics not affecting the interface is essential for the gate dielectric layer in future microelectronic devices.

Due to its elaborated controllability of thickness to the extent of atomic scale, atomic layer deposition (ALD) can be regarded as the excellent candidate for the deposition technique to produce thin films with atomically modulated compositional depth profiles. Recently, we reported the nitrogen depth profile control by in situ nitridation during plasma-enhanced atomic layer deposition (PE-ALD) for the HfO_2 layer growth with nitrogen/oxygen mixture plasma.[7] The electrical and interface properties were significantly improved when the nitrogen atoms are located in the middle of the HfO_2 films based on the angle-resolved X-ray photoelectron spectroscopy (AR-XPS) and capacitance–voltage (C-V) measurements. When the O/N mixture plasma was employed in PE-ALD, however, incorporated nitrogen contents were limited to less than ≅ 4%, which is too small to achieve robust thermal stability, as shown in the previous report.[7] Further, for the higher nitrogen-incorporated insertion layer of HfO_xN_y (nitrogen fraction $y > 0.04$; $f_{N/O}$ plasma gas fraction in growth condition >4), a complete trilayer showed quite high interface state density (D_{it}) and larger hysteresis (≅ 80 mV) than that (≅ 30 mV) of HfO_2 films.[7]

In the nitridation process, it is crucial to control nitrogen-related defects. High nitrogen incorporation into the interface has been generally thought to be detrimental to electrical properties of gate oxides by increasing the interface states through N–O and N–N bonding or interstitial N formation.[8] These nitrogen-related bonding states (N–O or N–N, etc.) usually form trap charge states in the HfO_xN_y thin film.[9] Previously, near-edge X-ray absorption fine-structure (NEXAFS) analysis has revealed the presence of a large number of N–N bonds in nitrided oxide films formed by high temperature annealing.[10] Thus, to improve the electrical properties of nitrided gate oxides, the removal of these unnecessary bonds is essential and a fabrication method for nitrogen depth profile control is strongly desired for high-k gate dielectrics in future microelectronic devices. In this paper, we report on the improved electrical properties of the $HfO_2/HfN/HfO_2$ (HfONO) trilayer, which is formed using H plasma as a reactant during PE-ALD.

Experimental

For this study, the PE-ALD system (Quros 200) was used for the deposition of the HfONO trilayer. Tetrakis(dimethylamino)hafnium was used as a Hf precursor and H_2 plasma was used as a reactant in the HfN PE-ALD system. The growth rates of ALD HfO_2 and HfN were 1.7 and 1 Å/cycle, respectively, by measuring the thickness of each sample deposited for 300 ALD cycles using an ellipsometry. The 1.3 nm thick HfO_2 layer in contact with the silicon channel region was deposited by PE-ALD in O_2 plasma ambient for 7 cycles, followed by HfN layer (2.5 nm) deposition for 25 cycles in H plasma ambient. An additional 7 cycles of HfO_2 deposition with the same growth condition as an introlayer were employed to cover the nitride layer. Separately, the HfO_2 layer with the same thickness was prepared for reference sample.

The impurity contents and chemical binding structures were analyzed by AR-XPS. The recrystallization temperature was determined by X-ray diffraction (XRD) analyses in postannealing experiments on as-deposited amorphous layers in N_2 ambient for 1 min at 500–800°C. The electronic structures of thin films were comparatively investigated using synchrotron analysis techniques, including X-ray photoemission spectroscopy (XPS) and NEXAFS analyses. The photoelectron spectroscopy was performed without surface sputtering at 90° of light incidence angle. To enable the microstruc-

* Electrochemical Society Active Member.
z E-mail: hyungjun@postech.ac.kr

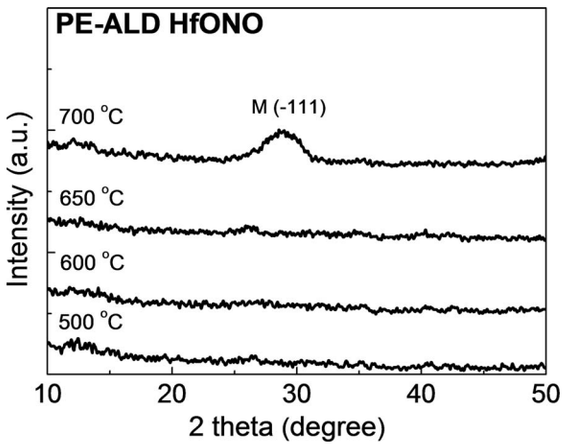

Figure 1. XRD data of HfONO after high temperature annealing.

ture and chemical composition analysis in nanoscale, high resolution C_s-corrected scanning transmission electron microscopy (STEM) (JEOL JEM-2100F) with energy-dispersive spectroscopy (EDS) was employed. The STEM was operated at 200 kV and its probe size was reduced to 0.1 nm for precise EDS analyses.

The films were deposited on p-type Si(001) substrates, which were cleaned at 70°C for 10 min in RCA solution [1:1:5 (v/v/v) $NH_4OH/H_2O_2/H_2O$] followed by dipping in buffered oxide enchant solution for 30 s to remove native oxide. For metal-oxide-semiconductor (MOS) capacitor fabrication, Ru was deposited by magnetron sputtering as a gate metal through a patterned shadow mask with a radius of 150 μm. Thermal-evaporated Au was used as a back contact. Postdeposition annealing and forming-gas annealing were carried out at 400°C for 10 min in an oxygen environment and for 30 min in H_2 5%–N_2 95%, respectively, to reduce trap charges. *C-V* and current–voltage characteristics were determined by using a Keithley 4200 semiconductor parameter analyzer with an HP4284 *LCR* meter. The capacitors were swept from inversion (+2.5 V) to accumulation (−2.5 V) and back to check the amount of the *C-V* hysteresis.

The interface state density (D_{it}) was determined by a conductance method carried out at various frequencies from 1 kHz to 1 MHz. Conductance G_p vs voltage and frequency was measured. The measured G_p value was corrected by taking into account the series resistance and insulator capacitance.[11] The conductance loss (G_p/ω) was selected at a maximum value in swept voltage. The D_{it} value was extracted by the following equation[12]

$$D_{it} = \left(\frac{G_p}{\omega}\right)_{max} [qf_D(\sigma_s)A]^{-1} \quad [1]$$

where G_p/ω is the corrected conductance loss, ω is the angular frequency ($\omega = 2\pi f$, f is the measurement frequency), q is the electronic charge (1.6×10^{19} C), f_D is the universal function as a function of standard deviation of band banding σ_s, and A is an area of the metal gate. For HfO_2, the f_D is 0.35–0.4.[12] To study the negative bias temperature instability (NBTI) characteristics, the −3 V voltage stress was applied for 3 min at room temperature to 125°C. After the voltage stresses, the V_{FB} shift and variations in D_{it} were measured. From the relationship of $\Delta N_p = -C_{ox}\Delta V_{FB}/q$, the trapped positive charge-density change (ΔN_p) was calculated. From the relationship of $\Delta N_p = -C_{ox}\Delta V_{FB}/q$, the trapped positive charge-density change (ΔN_p) was calculated.

Results

Figure 1 shows typical XRD θ-2θ scans from HfONO layers deposited on Si substrates, followed by an annealing process in N_2 atmosphere for 5 min at 500, 600, 650, and 750°C. For a separately

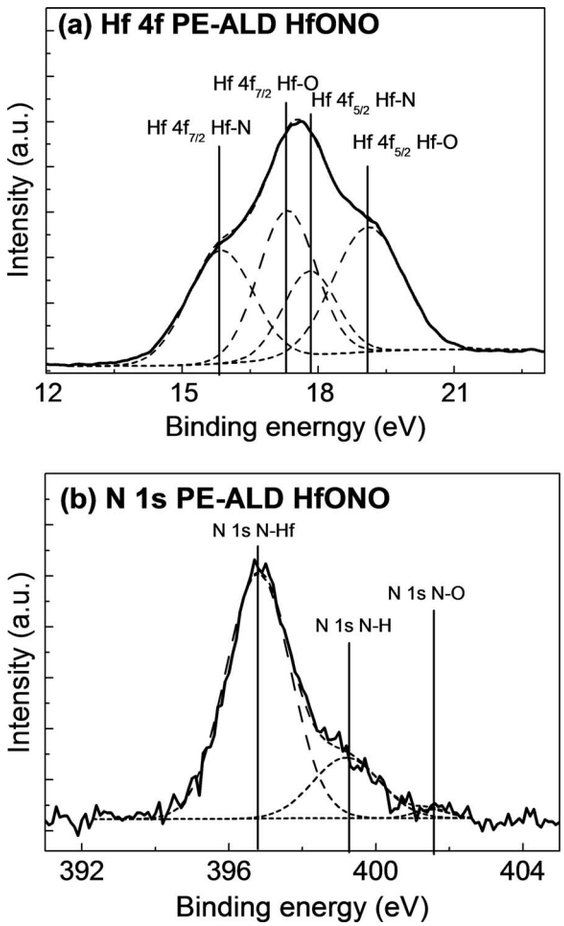

Figure 2. (a) Hf 4f and (b) N 1s XPS spectra of the HfONO sample.

prepared HfO_2 layer deposited by the PE-ALD system, recrystallization was observed at the annealing temperature around 500°C, revealing the XRD peak at 29° for the monoclinic structure of HfO_2 ($\bar{1}11$). However, Fig. 1 shows that the HfONO film still remains amorphous up to 650°C and finally generates a monoclinic HfO_2 ($\bar{1}11$) peak around 29–30° at the temperature of 700°C. An increase in recrystallization temperature of HfO_xN_y films with 15% nitrogen content was previously reported.[13] The recrystallization temperature of the HfONO sample in the present study has been increased by approximately 200°C compared to that of the pure layer, indicating the enhanced thermal stability against the recrystallization. The recrystallization produces a grain boundary, which is a major path for leakage current in gate dielectric. A separately prepared PE-ALD HfN film using H_2 plasma has shown an XRD peak of cubic HfN (111) at 34.5° and HfN (200) at 39.5° (data not shown). However, HfONO did not have those peaks, indicating that the nitride layer between HfO_2 layers was entirely oxidized during the deposition of the upper oxide layer, resulting in the formation of HfO_xN_y.

The chemical bonding states of samples were investigated in detail by XPS analyses. In our previous study, the XPS spectrum of HfO_2 was almost entirely composed of Hf–O bonds and did not have any impurity such as nitrogen- or carbon-related peaks, indicating the high purity of the films.[14] Figure 2a and b shows the representative Hf 4f and N 1s peaks of XPS analyses on the HfONO layers grown by PE-ALD using H_2 plasma, respectively. The nitrogen concentrations are 12 atom % from the XPS analysis. XPS of HfONO layers as shown in Fig. 2 revealed clear and distinct Hf–N bond-related peaks at 15.8 eV, 17.8 eV in Hf 4f, and 397 eV in N 1s,

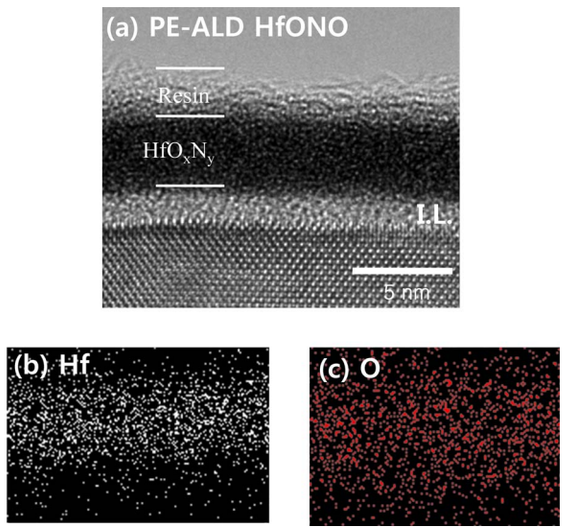

Figure 3. (Color online) (a) The TEM image of the Si/HfONO film, (b) elemental mapping by EDS analysis of the film (point: Hf), and (c) elemental mapping by EDS analysis of the film (point: O).

showing the formation of N–Hf bonds.[15] This result clearly indicates that the in situ nitrogen incorporation during PE-ALD was achieved by the current process. While conventional nitridation techniques to nitride the HfO_2 film require high temperature annealing (700°C) or plasma nitridation,[3] the current method employs the low process temperature because the nitridation layer is formed by direct deposition. The peak for N–H bonds at 399.2 eV was also observed.[16] A very small N–O bond was also detected at 401.5 eV.[7] However, the intensity of the N–O bond is much lower than that of our previous in situ nitridation method.[7]

Figure 3a is a typical bright-field transmission electron microscopy (TEM) image, showing the cross-sectional view of the HfONO layer grown on the Si substrate. The thickness of the film including the interfacial layer is approximately 5 nm. The nitrided middle layer is amorphous with a clean and smooth interface, which was formed by oxidization of the HfN during the upper HfO_2 layer deposition and subsequent annealing process. Figure 3b and c shows elemental maps obtained from the EDS analysis of the HfONO layer for Hf and O, respectively. The EDS results with the TEM image verify that the HfONO film is totally amorphorized and oxygen atoms are evenly distributed in the entire film, which agrees with the XRD and XPS analyses.

Figure 4a shows the *C-V* curves of MOS capacitors for both PE-ALD HfO_2 and HfONO. The capacitance equivalent oxide thickness (CET) of HfONO (≈1.25 nm) was lower than that of HfO_2 (≈1.40 nm). The process for nitrogen incorporation to dielectrics by H_2 plasma PE-ALD effectively contributes to the reduction in CET and obtains high-*k*. The nitride layer in the middle of the dielectric film can act as the trap charge layer. If the nitride layer is thick enough to retain the nonoxidized nitride layer in spite of the following oxide deposition, the large hysteresis would be observed due to charge trap effect as in a floating gate device. In effect, the *C-V* characteristics of HfO_2(1 nm)/HfN(20 nm)/HfO_2(1 nm) multilevel dielectrics, which was separately prepared, showed about 130 mV hysteresis. However, our 5 nm thick HfONO layer showed only ≤30 mV hysteresis (too small to be identified in Fig. 4a), which is similar to that of the HfO_2 monolayer (5 nm). The inner HfN layer in the HfONO film in this study was so thin that it is mostly oxidized, forming HfO_xN_y and losing N–N bonds during the oxidation. Compared to the middle nitrided sample prepared by oxygen–nitrogen mixture plasma in our previous study,[7] *C-V* hysteresis has been reduced from ≈80 to ≤30 mV. This method does not produce

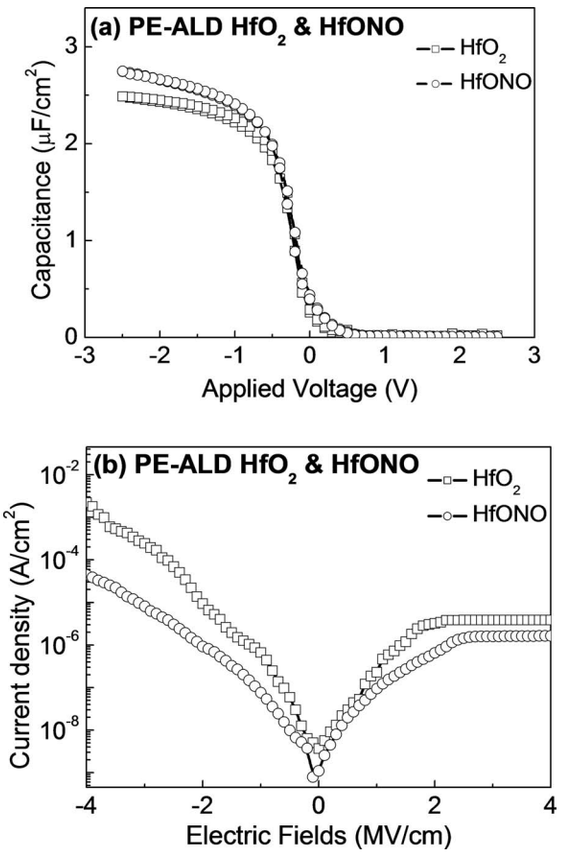

Figure 4. (a) The *C-V* curves and (b) the gate leakage currents of MOS capacitors with HfO_2 and HfONO as a gate insulator.

a V_{FB} shift in contrast to plasma nitridation which induced a significant negative V_{FB} shift ($\Delta V_{FB} = -80$ mV).[6] This difference is related to the low nitrogen incorporation into the interface due to the profile control of nitrogen. Figure 4b shows the leakage currents of MOS capacitors with HfO_2 and HfONO. The leakage currents of the HfONO sample are almost 12 times lower than that of HfO_2 at −1 MV/cm. This value (8×10^{-8} A/cm^2) is almost 2.5 times lower than that of our previous HfO_xN_y sample by N/O mixture plasma.[7]

Figure 5a and b shows the changes in trapped positive charge density (ΔN_p) and the changes in interface state density (ΔD_{it}) with increasing stress time, respectively. After 7 min of constant voltage stress, the ΔN_p of HfONO becomes two times lower than that of HfO_2 and the ΔD_{it} of HfONO becomes almost 30% lower than that of HfO_2. The NBTI immunity of the HfONO layer is more improved than that of the HfO_2 layer. The enhancement of the NBTI immunity can be attributed to the nitrogen incorporation combined with reduced defect states in the Hf-based oxide film.

To investigate the electronic structure of both HfO_2 and HfONO samples, valence-band spectra were studied using XPS analyses, as shown in Fig. 6a. The valence-band maxima (E_v) of HfO_2 and HfONO films were measured as −3.9 and −3.5 eV from Fermi energy, respectively, by a simple intersecting method.[17] The valence-band maximum of the HfONO layer is 0.4 eV higher than that of HfO_2. The lower valence-band offset [ΔE_v(Si–HfONO) = E_v(Si) − E_v(HfONO)] by nitrogen incorporation was previously reported in other research.[18] The conduction-band offset of HfONO was not decreased from the O K edge NEXAFS data of HfONO (shown in Fig. 6b). Figure 6c shows the N K edge spectrum of the HfONO sample. In the spectrum, two clearly different states of N are presented at approximately 405 and 400 eV.

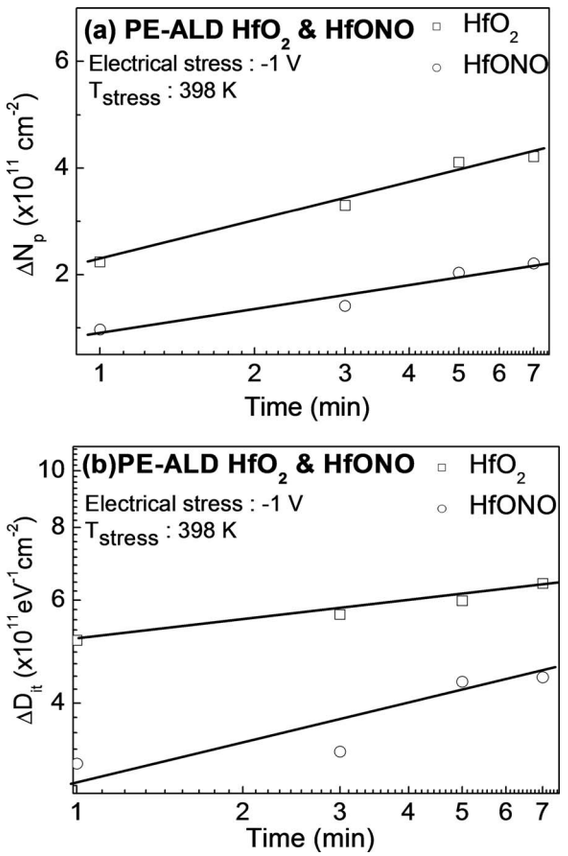

Figure 5. (a) Change in trapped positive charge density (ΔN_p) and (b) change in interface state density (ΔD_{it}) of HfO_2 and HfONO samples as a function of stress time under −1 V of constant voltage stress at 398 K.

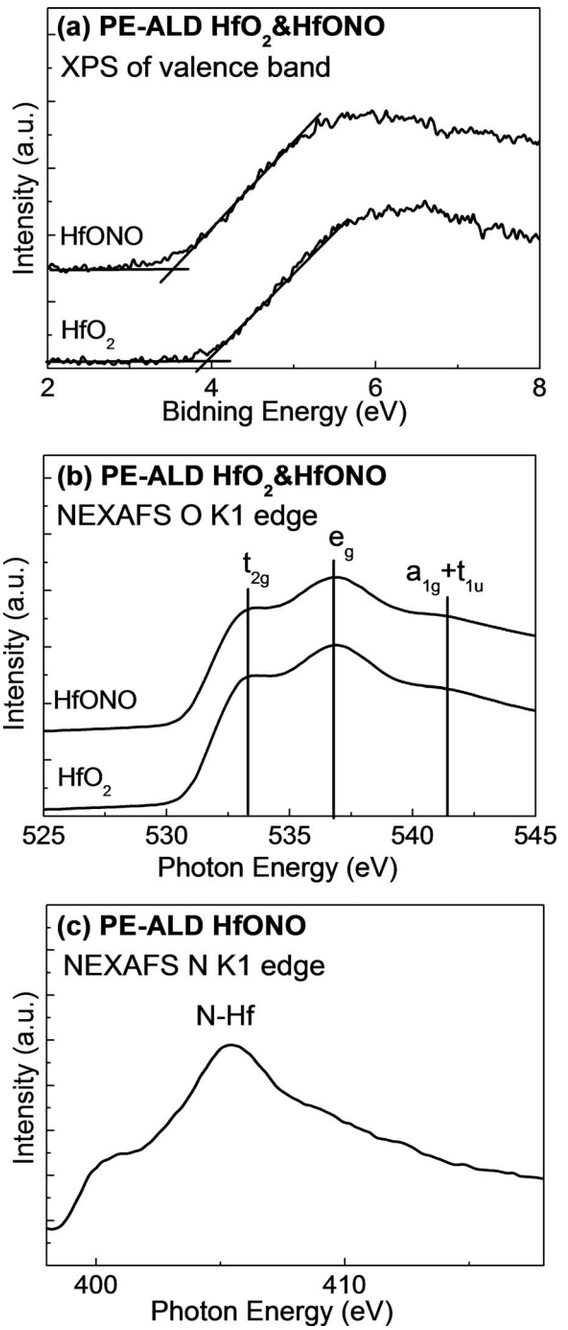

Figure 6. (a) Valence band and (b) O K1 edge of HfO_2 and HfONO. (c) N K1 edge NEXAFS spectra of the HfONO sample.

Discussion

From the experimental results, HfONO shows better film properties than HfO_2 such as lower CET, leakage currents, NBTI degradations, etc. Figure 6a shows that the valence-band maximum of HfONO is higher than that of HfO_2. From first-principles calculations, the N 2p states of Hf–N bonding are located above the valence-band maximum of HfO_2.[19,20] Although the valence-band offset decreases as nitrogen atoms incorporate due to the extension of N 2p states into the bandgap of HfO_2, the amount of the valence-band offset is large enough to act as a good hole barrier.[19,20] Thus, the leakage currents were not increased by incorporation of the middle nitride layer.

Given N K1 edge NEXAFS data (Fig. 6c), the peak at the higher energy region around 405 eV originated from the excitation from the Hf 6sp + N 2p states.[21] The lower intensity peak at approximately 401 eV represents the existence of N–H bonds,[22] which is in good agreement with the XPS analyses shown in Fig. 2b. The N–H bonding was formed by H_2 plasma during PE-ALD HfN in the current process. When nitrogen atoms are incorporated to gate oxide, it is apt to create nitrogen-related traps by N–N and N–O bonds which have a trap energy level below the conduction-band minimum; thus, nitrogen incorporation can induce conduction-band offset decrease and, in turn, undesirable high leakage currents. However, previous first-principles calculations (ab initio calculation) have shown that N–H bonding can reduce discrete and localized states below the conduction band available for carriers to be trapped during electrical excitation.[23] Also, N–H bonds can prevent the conduction-band lowering by enhancing the N 1s energy level, which is generally located under the conduction band without N–H bonds. Thus, N–H bonds can decrease the leakage currents, as seen in Fig. 4b. Thus, the nitrogen incorporation without forming N–O and N–N bonding by the current process with H_2 plasma can enhance the electrical properties due to the lower defect density without conduction-band lowering.

Figure 7 shows the schematic band diagram of the MOS structure for the (a) HfONO MOS structure, (b) bent energy diagrams under high electric field for the existence of trap states, (c) and state-free case, respectively. The N–H bonds in Hf-based gate oxide are efficient in blocking the leakage path for the metal gate. The work function of the Ru metal gate (5 eV) is referred to another previous study.[24] The gate leakage is dominant by electron tunneling

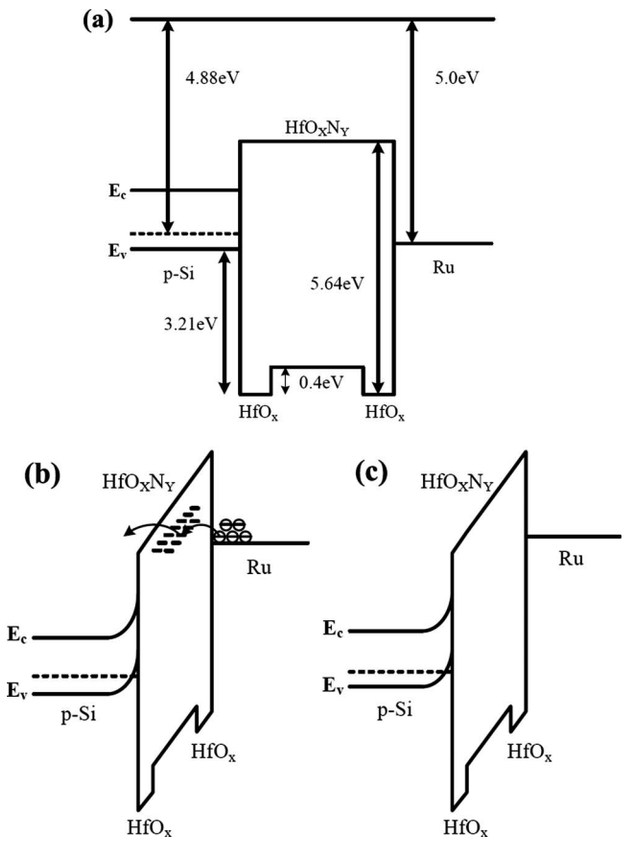

Figure 7. Schematic band diagram of the (a) MOS structures used in this experiment, (b) bended energy diagrams under high electric field for the existence of trap states, and (c) state-free case.

from the metal side under sufficient external bias. While the gate oxide with many trap states is weak for the electron tunneling illustrated in Fig. 7b, gate oxide which includes H–N bonds, suppressing conduction-band lowering, and reducing other trap sites such as N–N and N–O bonds, is secure to the tunneling. Therefore, the measured leakage currents of the HfONO layer showed even lower values than that of HfO_2 in spite of the lower valence-band offset.

Conclusions

The HfONO trilayer film, which was deposited using H_2 plasma as a reactant during PE-ALD, was systematically investigated. This sample showed lower values of interface trap density (D_{it}), trapped positive charge density (ΔN_p), and gate leakage currents than those of the HfO_2 monolayer, still sustaining comparable hysteresis and enhanced CET. These improved properties mainly result from the existence of N–H bonding, which raises the nitrogen 1s state level above the conduction minimum, hence compresses the generation of nitrogen-related defects and conduction-band lowering. Moreover, the decrement of N–O and N–N bonding that induces gap state and ascended recrystallization temperature further supported the betterment.

Acknowledgments

The XPS and NEXAFS were analyzed at the Pohang Accelerator Laboratory on beam line 4B1. This work was supported by Korea Ministry of Commerce, Industry and Energy (System IC 2010, Commercialization Program of Nano Process Equipments). Also, this work was supported by the Korea Science and Engineering Foundation (KOSEF) grant (no. R01-2007-000-20143-0, no. 2007-02864). Finally, this research was supported by WCU (World Class University) program through the Korea Science and Engineering Foundation funded by the Ministry of Education, Science and Technology (project no. R31-2008-000-10059-9).

Pohang University of Science and Technology assisted in meeting the publication costs of this article.

References

1. D. Buchanan, *IBM J. Res. Dev.*, **43**, 245 (1999).
2. K. Xiong, J. Robertson, and S. J. Clark, *J. Appl. Phys.*, **99**, 044105 (2006).
3. H. J. Cho, C. S. Kang, K. Onishi, S. Gopalan, R. Nieh, R. Choi, E. Dharmarajan, and J. C. Lee, *Tech. Dig. - Int. Electron Devices Meet.*, **2001**, 655.
4. K. Sekine, S. Inumiya, M. Sato, A. Kaneko, K. Eguchi, and Y. Tsunashima, *Tech. Dig. - Int. Electron Devices Meet.*, **2003**, 103.
5. E. P. Gusev, V. Narayanan, and M. M. Frank, *IBM J. Res. Dev.*, **50**, 387 (2006).
6. X. Yu, C. Zhu, and M. Yu, *Appl. Phys. Lett.*, **90**, 103502 (2007).
7. W. J. Maeng and H. Kim, *Appl. Phys. Lett.*, **91**, 092901 (2007).
8. E.-C. Lee, *Phys. Rev. B*, **77**, 104108 (2008).
9. J. L. Gavartin, A. L. Shluger, A. S. Foster, and G. I. Bersuker, *J. Appl. Phys.*, **97**, 053704 (2005).
10. K. B. Chung, C. N. Whang, M. H. Cho, C. J. Yim, and D. H. Ko, *Appl. Phys. Lett.*, **88**, 081903 (2006).
11. E. H. Nicollian and J. R. Brews, *MOS Physics and Technology*, Wiley Interscience, New Jersey (2003).
12. D.-G. Park, H.-J. Cho, K.-Y. Lim, C. Lim, I.-S. Yeo, J.-S. Roh, and J. W. Park, *J. Appl. Phys.*, **89**, 6275 (2001).
13. K. Chang Seok, H. J. Cho, K. Onishi, R. Choi, Y. H. Kim, R. Nieh, J. Han, S. Krishnan, A. Shahriar, and J. C. Lee, *Tech. Dig. - Int. Electron Devices Meet.*, **2002**, 865.
14. W. J. Maeng and H. Kim, *J. Electrochem. Soc.*, **155**, H267 (2008).
15. A. Arranz, *Surf. Sci.*, **563**, 1 (2004).
16. J. F. Moulder, W. F. Stickle, P. E. Sobol, and K. D. Bomben, *Handbook of X-Ray Photoelectron Spectroscopy: A Reference Book of Standard Spectra for Identification and Interpretation of XPS Data*, Perkin-Elmer, Minnesota (1992).
17. O. Renault, N. T. Barrett, D. Samour, and S. Quiais-Marthon, *Surf. Sci.*, **566**, 526 (2004).
18. X. J. Wang, L. D. Zhang, M. Liu, J. P. Zhang, and G. He, *Appl. Phys. Lett.*, **92**, 122901 (2008).
19. J. Choi, R. Puthenkovilakam, and J. P. Chang, *J. Appl. Phys.*, **99**, 053705 (2006).
20. G. Shang, P. W. Peacock, and J. Robertson, *Appl. Phys. Lett.*, **84**, 106 (2004).
21. J. G. Chen, *Surf. Sci. Rep.*, **30**, 1 (1997).
22. B. Bouchet-Fabre, K. Zellama, C. Godet, D. Ballutaud, and T. Minea, *Thin Solid Films*, **482**, 156 (2005).
23. D. Fischer, A. Curioni, S. Billeter, and W. Andreoni, *Phys. Rev. Lett.*, **92**, 236405 (2004).
24. T. Nabatame, K. Segawa, M. Kadoshima, H. Takaba, K. Iwamoto, S. Kimura, Y. Nunoshige, H. Satake, T. Ohishi, and A. Toriumi, *Mater. Sci. Semicond. Process.*, **9**, 975 (2006).